Hindawi
Journal of Applied Mathematics
Volume 2024, Article ID 7835548, 19 pages
https://doi.org/10.1155/2024/7835548

Research Article

Analytical Approximate Solutions of Caputo Fractional KdV-Burgers Equations Using Laplace Residual Power Series Technique

Aliaa Burqan,[1] **Mona Khandaqji**,[2] **Zeyad Al-Zhour**,[3] **Ahmad El-Ajou**,[4] **and Tasneem Alrahamneh**[4]

[1]*Department of Mathematics, Faculty of Science, Zarqa University, Zarqa 13110, Jordan*
[2]*Department of Mathematics, Applied Science Private University, Amman 11931, Jordan*
[3]*Department of Basic Engineering Sciences, College of Engineering, Imam Abdulrahman Bin Faisal University, Dammam 31441, Saudi Arabia*
[4]*Department of Mathematics, Faculty of Science, Al Balqa Applied University, Salt 19117, Jordan*

Correspondence should be addressed to Zeyad Al-Zhour; zeyad1968@yahoo.com

Received 17 February 2023; Revised 23 January 2024; Accepted 22 February 2024; Published 8 March 2024

Academic Editor: Fernando Simoes

The KdV-Burgers equation is one of the most important partial differential equations, established by Korteweg and de Vries to describe the behavior of nonlinear waves and many physical phenomena. In this paper, we reformulate this problem in the sense of Caputo fractional derivative, whose physical meanings, in this case, are very evident by describing the whole time domain of physical processing. The main aim of this work is to present the analytical approximate series for the nonlinear Caputo fractional KdV-Burgers equation by applying the Laplace residual power series method. The main tools of this method are the Laplace transform, Laurent series, and residual function. Moreover, four attractive and satisfying applications are given and solved to elucidate the mechanism of our proposed method. The analytical approximate series solution via this sweet technique shows excellent agreement with the solution obtained from other methods in simple and understandable steps. Finally, graphical and numerical comparison results at different values of α are provided with residual and relative errors to illustrate the behaviors of the approximate results and the effectiveness of the proposed method.

1. Introduction

Many events in chemistry, physics, biology, and other majors may be efficiently described using fractional calculus because accurate modeling of physical phenomena depends not only on immediate time but also on past time [1]. At this time, fractional calculus is growing in scale because it has unique and versatile properties [2]. The theory and applications of fractional F-PDEs have previously received many notable contributions [3]. These equations can be used, by researchers, more effectively to analyze and describe many phenomena in an assortment of fields, including mechanical and dynamical systems [4], pantograph equations [5], Navier-Stokes equations [6], and water wave propagation phenomena [7]. However, due to the complexity of the fractional calculus involving these equations, no approach provides an exact solution to the F-PDEs.

A variety of techniques is employed to solve several F-PDEs. The L-RPSM was created in 2020 by Eriqat et al. [5] to obtain the analytical approximate series solutions of the linear and nonlinear neutral fractional pantograph equations, and this method was subsequently used to investigate the exact and approximate (solitary, vector) solutions for various linear and nonlinear time-F-PDEs [8, 9]. The L-RPSM is constructed based on the LT and RPSM by transforming the differential equations to the Laplace space and then using an appropriate expansion to solve the new equation. The L-RPSM does not rely on the fractional derivation to determine the coefficients of the series as in RPSM but depends on the concept of the limit, so few calculations

generate the coefficients compared to RPSM. The current technique is quick, requires little computer memory, and is not influenced by computational round-off errors. Furthermore, this technique computes the coefficients of the power series using a chain of equations with more than one variable, indicating that the present method has a rapid convergence.

In the past two years, many works have employed the L-RPSM in providing accurate and approximate solutions to many F-PDEs, for example, fractional Fisher's equation and logistic system model [10], nonlinear fractional reaction-diffusion for bacteria growth model [11], fractional Lane-Emden equations [12], fuzzy quadratic Riccati FDE [13], a hyperbolic system of Caputo time-F-PDEs with variable coefficients [9], time-fractional Navier-Stokes equations [6], and time-fractional nonlinear water wave partial differential [7].

The KdV-BE was developed by Korteweg and de Vries [14], derived by Su and Gardner [15], and is used to describe nonlinear waves and many physical phenomena. It is also used to model problems established in many applied mathematics fields, including heat conduction, acoustic waves, gas dynamics, and traffic flow [16]. Nonlinear F-PDEs, such as fractional Burgers equations [17], F-KdV-BE [18], and fractional Schrödinger-KdV-BE [19], have also recently been proposed to explain some significant events and dynamic physics processes.

The homogeneous balancing method in [20], the truncated expansion method in [21], and the exponential function method in [22] were just a few of the several techniques used to obtain the exact solution of the KdV-BEs. Recently, many researchers have given more attention to the investigation of numerical techniques for solving KdV-BEs, such as the RPSM [23], Adomian decomposition method [24, 25], element-free Galerkin method [26], and explicit restrictive Taylor method [27].

Nonlinear fractional KdV-BEs are most commonly used in space-fractional or time-fractional derivative applications, according to studies [28, 29]. There are no applications for nonlinear fractional KdV-BEs that address the space-time-fractional state, and it is difficult to solve them using the established method, as described in the literature [28, 29], since it requires additional execution time to complete the approximation task.

The main objective of this work is to predict and create the ASSs for the following initial value Caputo FKdV-BE by using the L-RPSM:

$$\begin{aligned}&\mathfrak{D}_t^{\alpha}\psi(x,t)+\epsilon\psi^q(x,t)\mathfrak{D}_x^{\beta}\psi(x,t)+\eta\,\mathfrak{D}_x^2\psi(x,t)+\mu\,\mathfrak{D}_x^3\psi(x,t)\\&\quad=0,\ 0<\alpha,\beta\le 1,\ t,x>0,\\&\psi(x,0)=g(x),\end{aligned}\tag{1}$$

where $q=0,1,2$ and ϵ,η,μ are constants and α and β refer to the order of time-Caputo and space-CFD, respectively.

One of the main advantages of our proposed method (L-RPSM) is an efficient simple technique for finding exact and approximate series solutions to the linear and nonlinear F-PDEs compared with others such as residual power series, two-stage order-one Runge-Kutta, one-leg θ, variational iterative, Chebyshev polynomials method, Laguerre wavelet, Bernoulli wavelet, Boubaker polynomials, Hermit wavelet, and price-wise fractional-order Taylor methods. It must be noted that the study of the model's existence, uniqueness, and stability analysis of model (1) has been previously studied. The reader can refer to references [30, 31].

We arrange this paper as follows: In Section 2, we review some definitions and properties of some basic concepts and results related to the CFD, LT, and fractional Taylor and Laurent expansions, which are essential in constructing the L-RPS solutions for the FDEs. Section 3 gives an analytical solution of the nonlinear Caputo FKdV-BE based on the L-RPSM approach. In Section 4, the efficiency, effectiveness, and applicability of the L-RPSM are demonstrated by testing four nonlinear Caputo FKdV-BEs and comparing them with the results obtained in [23]. Finally, we summarize the outcomes of this paper in Conclusion.

2. Basic Concepts and Results

This section reviews some basic concepts and results related to the Caputo fractional operator, Laplace transform, and fractional Taylor and Laurent expansions which are essential in constructing the L-RPSM solutions for the FPDEs.

Definition 1. The fractional derivative of order $\alpha>0$ for the real-valued function $w(x,t)$ in the time-Caputo sense is denoted by $\mathfrak{D}_t^{\alpha}w(x,t)$ and defined as

$$\mathfrak{D}_t^{\alpha}w(x,t)=\begin{cases}J_t^{n-\alpha}\partial_t^n w(x,t),\ n-1<\alpha\le n,\ x\in K.t>0,\\ \partial_t^n w(x,t),\ \alpha=n,\end{cases}\tag{2}$$

where $\partial_t^n w(x,t)=\partial^n w(x,t)/\partial t^n$, $n\in\mathbb{N}$, K is an interval, and J_t^{α} is the time-Riemann-Liouville fractional integral of order α of the function $w(x,t)$ that defines as

$$J_t^{\alpha}w(x,t)=\begin{cases}\dfrac{1}{\Gamma(\alpha)}\displaystyle\int_0^t(t-\tau)^{\alpha-1}w(x,\tau)\,d\tau, & t>\tau>0,\\ w(x,\tau), & \alpha=0.\end{cases}\tag{3}$$

Note that the space-CFD is denoted and defined by the expression $\mathfrak{D}_x^{\alpha}w(x,t)=J_x^{n-\alpha}\partial_x^n w(x,t)$.

Definition 2 ([32]). Let $w(x,t)$ be a piecewise continuous function on $[0,\infty)$ and of exponential order δ. The LT of the $w(x,t)$ is denoted and given by

$$W(x,s)=\mathscr{L}[w(x,t)]=\int_0^{\infty}e^{-st}w(x,t)dt,\ s>\delta,\tag{4}$$

whereas the inverse LT of the function $W(x,s)$ is defined as

$$w(x,t) = \mathscr{L}^{-1}[W(x,s)] = \int_{z-i\infty}^{z+i\infty} e^{st} W(x,s)ds, z = \mathrm{Re}\,(s) > z_0. \tag{5}$$

The following Lemma gives the critical properties of the Laplace and inverse Laplace transformations required in this work.

Lemma 3 ([32]). *If $w(x,t)$ and $u(x,t)$ are piecewise continuous functions on the region $K \times [0,\infty)$ and of exponential orders δ_1 and δ_2, respectively, where $\delta_1 < \delta_2$. Suppose that $W(x,s) = \mathscr{L}[w(x,t)]$, $U(x,s) = \mathscr{L}[u(x,t)]$, and a, b are constants, then*

(i) $\mathscr{L}[aw(x,t) + bu(x,t)] = aW(x,s) + bU(x,s), x \in K, s > \delta_2$

(ii) $\mathscr{L}^{-1}[aW(x,s) + bU(x,s)] = aw(x,t) + bu(x,t), x \in K, t \geq 0$

(iii) $\lim_{s\longrightarrow\infty} sW(x,s) = w(x,0), x \in K$

(iv) $\mathscr{L}[\mathfrak{D}_t^{\alpha} w(x,t)] = s^{\alpha} W(x,s) - \sum_{k=0}^{n-1} s^{\alpha-k-1} \partial_t^k w(x,0), n - 1 < \alpha \leq n$

Theorem 4 (see [10]). *Let $w(x,t)$ be a piecewise continuous function on $K \times [0,\infty)$ and of exponential order δ. Suppose that the function $W(x,s) = \mathscr{L}[w(x,t)]$ has the following fractional power series:*

$$W(x,s) = \sum_{n=0}^{\infty} \frac{g_n(x)}{s^{n\alpha+1}}, 0 < \alpha \leq 1, x \in K, s > \delta. \tag{6}$$

Then, $g_n(x) = \mathfrak{D}_t^{n\alpha} w(x,0)$.

For more details regarding the convergence conditions for the fractional expansions, see [23].

Theorem 5 (see [10]). *Let $w(x,t)$ be a piecewise continuous function on $K \times [0,\infty)$ and of exponential order δ and $W(x,s) = \mathscr{L}[w(x,t)]$ can be represented as the fractional expansion in Theorem 4. If $|s\mathscr{L}[\mathfrak{D}_t^{(n+1)\alpha} w(x,t)]| \leq M(x)$ on $K \times (\delta,\gamma]$ where $0 < \alpha \leq 1$, then the remainder $R_n(x,s)$ of the fractional expansion as in Eq. (6) satisfies the following inequality:*

$$|R_n(x,s)| \leq \frac{M(x),}{s^{(n+1)\alpha+1}}, x \in K, \delta < s \leq \gamma. \tag{7}$$

3. L-RPSM Solutions to the Caputo FKdV-BE

This section provides an analytical solution for the Caputo FKdV-BE in Eq. (1) based on the L-RPS approach. Before we start with that and without losing the other cases, we will set the value of q to be 2, leaving the reader to repeat the same steps to reach the construction required for the solution in the other two cases, $q = 1$ and $q = 0$. Part (iv) of Lemma 3 produces the following equation when the LT is applied to both sides concerning t:

$$\Psi(x,s) - \frac{g(x)}{s} + \frac{\epsilon}{s^{\alpha}} \mathscr{L}_t\left[\left(\mathscr{L}_t^{-1}[\Psi(x,s)]\right)^2 \mathfrak{D}_x^{\beta}\left(\mathscr{L}_t^{-1}[\Psi(x,s)]\right)\right] + \frac{\eta}{s^{\alpha}} \mathfrak{D}_x^2 \Psi(x,s) + \frac{\mu}{s^{\alpha}} \mathfrak{D}_x^3 \Psi(x,s) = 0, \tag{8}$$

where $\Psi(x,s) = \mathscr{L}_t[\psi(x,t)], s > \delta \geq 0$.

According to Theorem 4, we assume the L-RPS approach dictates that the series solution of Eq. (8) takes the following fractional expansion:

$$\Psi(x,s) = \sum_{n=0}^{\infty} \frac{g_n(x)}{s^{n\alpha+1}}, x \in K, s > \delta \geq 0. \tag{9}$$

Since $\lim_{s\longrightarrow\infty} s\Psi(x,s) = \psi(x,0) = g(x)$, the kth truncated series solution of $\Psi(x,s)$ takes the following form:

$$\Psi_k(x,s) = \frac{g(x)}{s} + \sum_{n=1}^{k} \frac{g_n(x)}{s^{n\alpha+1}}, x \in I, s > \delta \geq 0, k = 1, 2, \cdots. \tag{10}$$

We define the Laplace residual function and the kth Laplace residual function, respectively, of Eq. (8) as follows:

$$\begin{aligned} LRes(x,s) = {} & \Psi(x,s) - \frac{g(x)}{s} \\ & + \frac{\epsilon}{s^{\alpha}} \mathscr{L}\left[\left(\mathscr{L}^{-1}[\Psi(x,s)]\right)^2 \mathfrak{D}_x^{\beta}\left(\mathscr{L}^{-1}[\Psi(x,s)]\right)\right] \\ & + \frac{\eta}{s^{\alpha}} \mathfrak{D}_x^2 \Psi(x,s) + \frac{\mu}{s^{\alpha}} \mathfrak{D}_x^3 \Psi(x,s) = 0, \end{aligned} \tag{11}$$

$$\begin{aligned} LRes_k(x,s) = {} & \Psi_k(x,s) - \frac{g(x)}{s} \\ & + \frac{\epsilon}{s^{\alpha}} \mathscr{L}\left[\left(\mathscr{L}^{-1}[\Psi_k(x,s)]\right)^2 \mathfrak{D}_x^{\beta}\left(\mathscr{L}^{-1}[\Psi_k(x,s)]\right)\right] \\ & + \frac{\eta}{s^{\alpha}} \mathfrak{D}_x^2 \Psi_k(x,s) + \frac{\mu}{s^{\alpha}} \mathfrak{D}_x^3 \Psi_k(x,s) \\ & = 0, k = 1, 2, 3, \cdots. \end{aligned} \tag{12}$$

The following are some relevant facts to determine the ASS according to the L-RPS technique, see [8]:

$$\begin{aligned} &\text{(i)} \quad \lim_{k\longrightarrow\infty} LRes_k(x,s) = LRes(x,s) = 0, x \in K, s > \delta \geq 0, \\ &\text{(ii)} \quad \lim_{s\longrightarrow\infty}\left(s^{k\alpha+1} LRes(x,s)\right) = \lim_{s\longrightarrow\infty}\left(s^{k\alpha+1} LRes_k(x,s)\right) \\ &\qquad = 0, 0 < \alpha \leq 1, k = 1, 2, 3,. \end{aligned} \tag{13}$$

Therefore, to obtain the unknown coefficients $g_n(x)$, we must first substitute the kth truncated series solution $\Psi_k(x,s)$ for $k=1,2,3,\cdots$, into the kth Laplace residual function in Eq. (12). Then, we solve $\lim_{s\longrightarrow\infty}(s^{k\alpha+1}LRes_k(x,s)) = 0$ and gather the acquired coefficients $g_n(x)$ in terms of fractional expansion series $\Psi_k(x,s)$. After that, we apply the inverse LT to both sides of the resulting Laplace series solution to get the ASS of the original problem in Eq. (1).

Now, $\Psi_1(x,s)$ is substituted into the first-residual function $LRes_1(x,s)$ to get

$$\begin{aligned} LRes_1(x,s) = {} & \frac{g_1(x)}{s^{\alpha+1}} + \frac{\epsilon}{s^\alpha}\mathscr{L}\left[\left(\mathscr{L}^{-1}\left[\frac{g(x)}{s}+\frac{g_1(x)}{s^{\alpha+1}}\right]\right)^2\right. \\ & \left.\cdot\,\mathfrak{D}_x^\beta\left(\mathscr{L}^{-1}\left[\frac{g(x)}{s}+\frac{g_1(x)}{s^{\alpha+1}}\right]\right)\right] \\ & + \frac{\eta}{s^\alpha}\mathfrak{D}_x^2\left(\frac{g(x)}{s}+\frac{g_1(x)}{s^{\alpha+1}}\right) + \frac{\mu}{s^\alpha}\mathfrak{D}_x^3\left(\frac{g(x)}{s}+\frac{g_1(x)}{s^{\alpha+1}}\right). \end{aligned} \tag{14}$$

The first coefficient $g_1(x)$ can be obtained by multiplying both sides of Eq. (14) by $s^{\alpha+1}$ and then by solving $\lim_{s\longrightarrow\infty} s^{\alpha+1} LRes_1(x,s) = 0$. Then, we have

$$g_1(x) = -\left(\epsilon g^2(x)\mathfrak{D}_x^\beta g(x) + \eta g''(x) + \mu g'''(x)\right). \tag{15}$$

Thus, the 1st truncated series solution can be expressed as

$$\Psi_1(x,s) = \frac{g(x)}{s} - \frac{\left(\epsilon g^2(x)\mathfrak{D}_x^\beta g(x)g(x) + \eta g''(x) + \mu g'''(x)\right)}{s^{\alpha+1}}. \tag{16}$$

Similar to how $g_1(x)$ was calculated, $g_2(x)$ is likewise calculated by inserting the 2nd truncated series $\Psi_2(x,s) = g(x)/s + g_1(x)/s^{\alpha+1} + g_2(x)/s^{2\alpha+1}$ into Eq. (12) to obtain

$$\begin{aligned} LRes_2(x,s) = {} & \frac{g_1(x)}{s^{\alpha+1}} + \frac{g_2(x)}{s^{2\alpha+1}} \\ & + \frac{\epsilon}{s^\alpha}\mathscr{L}\left[\left(\mathscr{L}^{-1}\left[\frac{g(x)}{s}+\frac{g_1(x)}{s^{\alpha+1}}+\frac{g_2(x)}{s^{2\alpha+1}}\right]\right)^2\right. \\ & \left.\cdot\,\mathfrak{D}_x^\beta\left(\mathscr{L}^{-1}\left[\frac{g(x)}{s}+\frac{g_1(x)}{s^{\alpha+1}}+\frac{g_2(x)}{s^{2\alpha+1}}\right]\right)\right] \\ & + \frac{\eta}{s^\alpha}\mathfrak{D}_x^2\left(\frac{g(x)}{s}+\frac{g_1(x)}{s^{\alpha+1}}+\frac{g_2(x)}{s^{2\alpha+1}}\right) \\ & + \frac{\mu}{s^\alpha}\mathfrak{D}_x^3\left(\frac{g(x)}{s}+\frac{g_1(x)}{s^{\alpha+1}}+\frac{g_2(x)}{s^{2\alpha+1}}\right). \end{aligned} \tag{17}$$

Next, multiply both sides of Eq. (17) by $s^{2\alpha+1}$, and then by solving $\lim_{s\longrightarrow\infty} s^{2\alpha+1}LRes_2(x,s) = 0$, one can get

$$\begin{aligned} g_2(x) = {} & -\left(\epsilon\left(2g(x)g_1(x)\mathfrak{D}_x^\beta g(x) + g^2(x)\mathfrak{D}_x^\beta g_1(x)\right)\right. \\ & \left. + \eta g_1''(x) + \mu g_1'''(x)\right). \end{aligned} \tag{18}$$

So, the 2nd truncated series solution of Eq. (8) is given as

$$\begin{aligned} \Psi_2(x,s) = {} & \frac{g(x)}{s} - \frac{\left(\epsilon g^2(x)\mathfrak{D}_x^\beta g(x)g(x) + \eta g''(x) + \mu g'''(x)\right)}{s^{\alpha+1}} \\ & - \frac{\epsilon\left(2g(x)g_1(x)\mathfrak{D}_x^\beta g(x) + g^2(x)\mathfrak{D}_x^\beta g_1(x)\right) + \eta g_1''(x) + \mu g_1'''(x)}{s^{2\alpha+1}}. \end{aligned} \tag{19}$$

The following results are also easily obtained for $k=3$ by following the same procedure as above:

$$\begin{aligned} g_3(x) = {} & -\left(\epsilon\left(2g_1^2(x)\mathfrak{D}_x^\beta g(x) + 4g(x)g_1(x)\mathfrak{D}_x^\beta g_1(x) + 2g(x)g_2(x)\mathfrak{D}_x^\beta g(x)\right.\right. \\ & \left.\left. + g^2(x)\mathfrak{D}_x^\beta g_2(x)\right) + \eta g_2''(x) + \mu g_2'''(x)\right). \end{aligned} \tag{20}$$

In fact, the 3rd truncated series solution of Eq. (8), based on the prior findings of $g_1(x)$, $g_2(x)$, and $g_3(x)$, is provided by

$$\begin{aligned} \Psi_3(x,s) = {} & \frac{g(x)}{s} - \frac{\left(\epsilon g^2(x)\mathfrak{D}_x^\beta g(x)g(x) + \eta g''(x) + \mu g'''(x)\right)}{s^{\alpha+1}} \\ & - \frac{\epsilon\left(2g(x)g_1(x)\mathfrak{D}_x^\beta g(x) + g^2(x)\mathfrak{D}_x^\beta g_1(x)\right) + \eta g_1''(x) + \mu g_1'''(x)}{s^{2\alpha+1}} \\ & - \frac{\epsilon\left(2g_1^2(x)\mathfrak{D}_x^\beta g(x) + 4g(x)g_1(x)\mathfrak{D}_x^\beta g_1(x) + 2g(x)g_2(x)\mathfrak{D}_x^\beta g(x) + g^2(x)\mathfrak{D}_x^\beta g_2(x)\right) + \eta g_2''(x) + \mu g_2'''(x)}{s^{3\alpha+1}}. \end{aligned} \tag{21}$$

One may derive $g_k(x)$ for $k = 4, 5, 6, \cdots$ by processing the preceding stages and utilizing the solution of the system $\lim_{s\longrightarrow\infty} s^{k\alpha+1} LRes_k(x,s) = 0$. Then, we get the kth truncated series solution $\Psi_k(x,s)$ as follows:

$$\begin{aligned}\Psi_k(x,s) = {} & \frac{g(x)}{s} - \frac{\left(\epsilon g^2(x)\mathfrak{D}_x^\beta g(x)g(x) + \eta g''(x) + \mu g'''(x)\right)}{s^{\alpha+1}} \\ & - \frac{\epsilon\left(2g(x)g_1(x)\mathfrak{D}_x^\beta g(x) + g^2(x)g_1^{(\beta)}(x)\right) + \eta g_1''(x) + \mu g_1'''(x)}{s^{2\alpha+1}} \\ & - \frac{\epsilon\left(2g_1^2(x)\mathfrak{D}_x^\beta g(x) + 4g(x)g_1(x)\mathfrak{D}_x^\beta g_1(x) + 2g(x)g_2(x)\mathfrak{D}_x^\beta g(x) + g^2(x)\mathfrak{D}_x^\beta g_2(x)\right) + \eta g_2''(x) + \mu g_2'''(x)}{s^{3\alpha+1}} - \cdots - \frac{g_k(x)}{s^{k\alpha+1}}.\end{aligned} \tag{22}$$

In the following step, we operate the inverse LT to both sides of Eq. (22) to get the kth ASS of the initial value problem of the Caputo FKdV-BE of Eq. (1) as follows:

$$\begin{aligned}\psi_k(x,t) = {} & g(x) - \frac{\left(\epsilon g^2(x)\mathfrak{D}_x^\beta g(x)g(x) + \eta g''(x) + \mu g'''(x)\right)}{\Gamma(\alpha+1)} t^\alpha \\ & - \frac{\epsilon\left(2g(x)g_1(x)\mathfrak{D}_x^\beta g(x) + g^2(x)\mathfrak{D}_x^\beta g_1(x)\right) + \eta g_1''(x) + \mu g_1'''(x)}{\Gamma(2\alpha+1)} t^{2\alpha} \\ & - \frac{\epsilon\left(2g_1^2(x)g(x) + 4g(x)g_1(x)\mathfrak{D}_x^\beta g_1(x) + 2g(x)g_2(x)\mathfrak{D}_x^\beta g(x) + g^2(x)\mathfrak{D}_x^\beta g_2(x)\right) + \eta g_2''(x) + \mu g_2'''(x)}{\Gamma(3\alpha+1)} t^{3\alpha} - \cdots. \\ & - \frac{g_k(x)}{\Gamma(k\alpha+1)} t^{k\alpha}.\end{aligned} \tag{23}$$

Finally, the ASS of the Caputo FKdV-BE of Eq. (1) is given by

$$\begin{aligned}\psi(x,t) = \lim_{k\longrightarrow\infty} \psi_k(x,t) = {} & g(x) - \frac{\left(\epsilon g^2(x)\mathfrak{D}_x^\beta g(x)g(x) + \eta g''(x) + \mu g'''(x)\right)}{\Gamma(\alpha+1)} t^\alpha \\ & - \frac{\epsilon\left(2g(x)g_1(x)\mathfrak{D}_x^\beta g(x) + g^2(x)\mathfrak{D}_x^\beta g_1(x)\right) + \eta g_1''(x) + \mu g_1'''(x)}{\Gamma(2\alpha+1)} t^{2\alpha} \\ & - \frac{\epsilon\left(2g_1^2(x)g(x) + 4g(x)g_1(x)\mathfrak{D}_x^\beta g_1(x) + 2g(x)g_2(x)\mathfrak{D}_x^\beta g(x) + g^2(x)\mathfrak{D}_x^\beta g_2(x)\right) + \eta g_2''(x) + \mu g_2'''(x)}{\Gamma(3\alpha+1)} t^{3\alpha} - \cdots.\end{aligned} \tag{24}$$

Using the same procedure as before, we can discover ASSs to the same Caputo FKdV-BE of Eq. (1) in the case of $q = 1$ and $q = 0$ as we mentioned above.

When $q=1$, the initial coefficients of the kth truncated series solution to Eq. (1) are:

$$g_0(x)=g(x), \tag{25}$$

$$\begin{aligned}
g_1(x)&=-\left(\epsilon g(x)\mathfrak{D}_x^\beta g(x)+\eta g''(x)+\mu g'''(x)\right),\\
g_2(x)&=-\left(\epsilon\left(g_1(x)\mathfrak{D}_x^\beta g(x)+g(x)\mathfrak{D}_x^\beta g_1(x)\right)+\eta g_1''(x)+\mu g_1'''(x)\right),\\
g_3(x)&=-\left(\epsilon\left(g_2(x)\mathfrak{D}_x^\beta g(x)+2g_1(x)\mathfrak{D}_x^\beta g_1(x)+g(x)\mathfrak{D}_x^\beta g_2(x)\right)\right.\\
&\quad\left.+\eta g_2''(x)+\mu g_2'''(x)\right),\\
&\vdots\,.
\end{aligned} \tag{26}$$

Whereas for $q=0$, the first four coefficients will be as follows:

$$\begin{aligned}
g_0(x)&=g(x),\\
g_1(x)&=-\left(\epsilon\mathfrak{D}_x^\beta g(x)+\eta g''(x)+\mu g'''(x)\right),\\
g_2(x)&=-\left(\epsilon\mathfrak{D}_x^\beta g_1(x)+\eta g_1''(x)+\mu g_1'''(x)\right),\\
g_3(x)&=-\left(\epsilon\mathfrak{D}_x^\beta g_2(x)+\eta g_2''(x)+\mu g_2'''(x)\right),\\
&\vdots\,.
\end{aligned} \tag{27}$$

In the next section, we utilize the obtained coefficients in Eqs. (23), (25), and (27) to introduce ASSs to four examples of time, space, and time-space Caputo FKdV-BE.

4. Some Attractive Applications

In this section, the efficiency, effectiveness, and applicability of the L-RPSM are demonstrated by testing four nonlinear Caputo FKdV-BE initial value problems and comparing them with the results in [23]. It should be noted that the MATHEMATICA 12 software package is used for all numerical and symbolic operations.

Application 6. Consider the following nonlinear time-Caputo FKdV-BE

$$\begin{aligned}
&\mathfrak{D}_t^\alpha\psi(x,t)+6\psi^2(x,t)\mathfrak{D}_x\psi(x,t)+\mathfrak{D}_x^3\psi(x,t)=0, x\in K, t>0, 0<\alpha\le 1,\\
&\psi(x,0)=\sqrt{c}\,\mathrm{sech}\left(\omega+\sqrt{c}x\right).
\end{aligned} \tag{28}$$

Comparing Eq. (28) with Eq. (1), we find that $q=2$, $\beta=1$, $\epsilon=6$, $\eta=0$, and $\mu=1$ with the initial condition $g_0(x)=\sqrt{c}\,\mathrm{sech}\,(\omega+\sqrt{c}x)$, where c and ω are constants. As a result, using the methodology described in Section 3, the LT of Eq. (28) is

$$\begin{aligned}
&\Psi(x,s)-\frac{\sqrt{c}\,\mathrm{sech}\left(\omega+\sqrt{c}x\right)}{s}\\
&\quad+\frac{6}{s^\alpha}\mathscr{L}_t\left[\left(\mathscr{L}_t^{-1}[\Psi(x,s)]\right)^2\mathfrak{D}_x\left(\mathscr{L}_t^{-1}[\Psi(x,s)]\right)\right]\\
&\quad+\frac{1}{s^\alpha}\mathfrak{D}_x^3\Psi(x,s)=0,
\end{aligned} \tag{29}$$

the ASS of Eq. (29) is

$$\Psi(x,s)=\sum_{n=0}^{\infty}\frac{g_n(x)}{s^{n\alpha+1}}, x\in K, s>\delta\ge 0, \tag{30}$$

and consequently the kth truncated series of $\Psi(x,s)$ will be

$$\Psi_k(x,s)=\frac{\sqrt{c}\,\mathrm{sech}\left(\omega+\sqrt{c}x\right)}{s}+\sum_{n=1}^{k}\frac{g_n(x)}{s^{n\alpha+1}}, k=1,2,\cdots. \tag{31}$$

According to the results in Eqs. (15), (18), and (20), we derive $g_n(x)$ for $n=1$, 2, and 3 as:

$$\begin{aligned}
g_1(x)&=c^2\tanh\left(\omega+\sqrt{c}x\right)\mathrm{sech}\left(\omega+\sqrt{c}x\right),\\
g_2(x)&=-\frac{1}{2}c^{7/2}\,\mathrm{sech}^3\left(\omega+\sqrt{c}x\right)\left(3-\cosh\left(2\left(\omega+\sqrt{c}x\right)\right)\right),\\
g_3(x)&=-\frac{c^5}{8}\,\mathrm{sech}^5\left(\omega+\sqrt{c}x\right)\tanh\left(\omega+\sqrt{c}x\right)\frac{24\Gamma(1+2\alpha)}{\Gamma(1+\alpha)^2}\\
&\quad\cdot\left(7-3\cosh\left(2\left(\omega+\sqrt{c}x\right)\right)\right)+315-164\cosh\left(2\left(\omega+\sqrt{c}x\right)\right)\\
&\quad+\cosh\left(4\left(\omega+\sqrt{c}x\right)\right).
\end{aligned} \tag{32}$$

Then, the 3rd truncated series in Eq. (31) becomes

$$\begin{aligned}
\Psi_3(x,s)&=\frac{\sqrt{c}\,\mathrm{sech}\left(\omega+\sqrt{c}x\right)}{s}+\frac{c^2\tanh\left(\omega+\sqrt{c}x\right)\mathrm{sech}\left(\omega+\sqrt{c}x\right)}{s^{\alpha+1}}\\
&\quad-\frac{c^{7/2}}{2}\frac{\mathrm{sech}^3\left(\omega+\sqrt{c}x\right)\left(3-\cosh 2\left(\omega+\sqrt{c}x\right)\right)}{s^{2\alpha+1}}\\
&\quad-\frac{c^5}{8}\,\mathrm{sech}^5\left(\omega+\sqrt{c}x\right)\tanh\left(\omega+\sqrt{c}x\right)\frac{24\Gamma(1+2\alpha)}{\Gamma(1+\alpha)^2}\\
&\quad\cdot\left(7-3\cosh 2\left(\omega+\sqrt{c}x\right)\right)+315-164\cosh 2\left(\omega+\sqrt{c}x\right)\\
&\quad+\cosh 4\left(\omega+\sqrt{c}x\right)\frac{1}{s^{3\alpha+1}}.
\end{aligned} \tag{33}$$

Consequently, the 3rd approximate L-RPS solution of Eq. (28) takes the following expansions:

$$\begin{aligned}\psi_3(x,t) = {} & \sqrt{c}\,\operatorname{sech}\left(\omega+\sqrt{c}x\right) \\ & + c^2 \tanh\left(\omega+\sqrt{c}x\right)\operatorname{sech}\left(\omega+\sqrt{c}x\right)\frac{t^{\alpha}}{\Gamma(1+\alpha)} \\ & - \frac{1}{2}c^{7/2}\operatorname{sech}^3\left(\omega+\sqrt{c}x\right) \\ & \cdot\left(3-\cosh\left(2\left(\omega+\sqrt{c}x\right)\right)\right)\frac{t^{2\alpha}}{\Gamma(1+2\alpha)} \\ & + \left(\frac{c^5}{8}\frac{24\Gamma(1+2\alpha)}{\Gamma(1+\alpha)^2}\tanh\left(\omega+\sqrt{c}x\right)\operatorname{sech}^5\left(\omega+\sqrt{c}x\right)\right. \\ & \cdot\left(-7+3\cosh\left(2\left(\omega+\sqrt{c}x\right)\right)\right)+315+\cosh\left(4\left(\omega+\sqrt{c}x\right)\right) \\ & - 164\cosh\left(2\left(\omega+\sqrt{c}x\right)\right)\Big)\frac{t^{3\alpha}}{\Gamma(1+3\alpha)}.\end{aligned} \tag{34}$$

The authors introduced in [23] an approximate RPSM solution for Eq. (28), where the obtained 3rd ASS coincided with $\psi_3(x,t)$ in Eq. (34).

Remark 7. The solution of Eq. (28) has a general form that coincides with the following exact solution when $\alpha = 1$.

$$\psi(x,t) = \sqrt{c}\,\operatorname{sech}\left(\omega+\sqrt{c}(x-ct)\right). \tag{35}$$

To demonstrate the geometric behaviors of the L-RPS solution of Eq. (28) and the range of its accuracy, a comparison between the approximate solution $\psi_3(x,t)$ and exact solution $\psi(x,t)$ is given in 3D for a different value of α and $c = 1, \omega = 0$, see Figure 1. From Figure 1, it is clear that the behaviors of the subfigures are almost identical and coincidental, especially for Figures 1(c) and 1(d) where $\alpha = 1$. These subfigures appear identical and in perfect agreement in terms of accuracy with each other. As a result, compared to the exact solution, computing a few terms can yield an outstanding approximation. Consequently, the overall error can vanish by finding a larger number of the series terms.

To confirm this, numerical values for the actual and the relative errors of the approximation $\psi_3(x,t)$ are calculated in Table 1 when $\alpha = 1$. Table 2 shows the residual error of the approximation $\psi_3(x,t)$ when $\alpha = 0.80$ and 0.90. The numerical results show that the obtained approximation is acceptable mathematically. The actual and relative errors are defined, respectively, as follows:

$$\begin{aligned}\text{Actual error} &= \left|\psi(x,t)-\psi_k(x,t)\right|, \\ \text{Relative error} &= \left|\frac{\psi(x,t)-\psi_k(x,t)}{\psi(x,t)}\right|,\end{aligned} \tag{36}$$

while the residual error for the problem in Eq. (28) is given by:

$$\text{Residual error}\,(x,t) = \left|\frac{\partial^{\alpha}\psi_k(x,t)}{\partial t^{\alpha}} + \epsilon\psi_k^{r}(x,t)\frac{\partial^{\beta}\psi_k(x,t)}{\partial x^{\beta}} + \eta\frac{\partial^2\psi_k(x,t)}{\partial x^2} + \mu\frac{\partial^3\psi_k(x,t)}{\partial x^3}\right|. \tag{37}$$

Application 8. Consider the nonlinear time-Caputo FKdV-BE

$$\begin{aligned}&\mathfrak{D}_t^{\alpha}\psi(x,t) - 6\psi(x,t)\mathfrak{D}_x\psi(x,t) + \mathfrak{D}_x^3\psi(x,t) = 0, x, t > 0, 0 < \alpha \le 1, \\ &\psi(x,0) = \frac{-2\omega^2 e^{\omega x}}{\left(1+e^{\omega x}\right)^2}.\end{aligned} \tag{38}$$

As we discussed in the previous application, comparing Eq. (38) with Eq. (1), we find that $q = \mu = \beta = 1$, $\epsilon = -6$, and $\eta = 0$ with the initial condition $g_0(x) = -2\omega^2 e^{\omega x}/(1+e^{\omega x})^2$, where ω is a constant. Therefore, according to the working mechanism of the L-RPSM, we transfer Eq. (1) to the Laplace space as

$$\begin{aligned}\Psi(x,s) &+ \frac{2\omega^2 e^{\omega x}}{\left(1+e^{\omega x}\right)^2}\frac{1}{s} - \frac{6}{s^{\alpha}}\mathscr{L}_t\left[\left(\mathscr{L}_t^{-1}[\Psi(x,s)]\right)\mathfrak{D}_x\left(\mathscr{L}_t^{-1}[\Psi(x,s)]\right)\right] \\ &+ \frac{1}{s^{\alpha}}\mathfrak{D}_x^3\Psi(x,s) = 0,\end{aligned} \tag{39}$$

where $s > \delta \ge 0$, assume the solution of Eq. (39) in the following form:

$$\Psi(x,s) = \sum_{n=0}^{\infty}\frac{g_n(x)}{s^{n\alpha+1}}, x \in K, s > \delta \ge 0, \tag{40}$$

and the kth truncated series of $\Psi(x,s)$ will be

$$\Psi_k(x,s) = \frac{-2\omega^2 e^{\omega x}}{\left(1+e^{\omega x}\right)^2}\frac{1}{s} + \sum_{n=1}^{k}\frac{g_n(x)}{s^{n\alpha+1}}, k = 1, 2, \cdots. \tag{41}$$

According to the results in Eqs. (15), (18), and (20), we set $g_n(x)$, $n = 1, 2, 3$ as follows:

$$g_1(x) = \frac{-2e^{\omega x}\left(e^{x\omega}-1\right)\omega^5}{\left(1+e^{\omega x}\right)^3},$$

$$g_2(x) = \frac{-2e^{\omega x}\left(1-4e^{\omega x}+e^{2\omega x}\right)\omega^8}{\left(1+e^{\omega x}\right)^4},$$

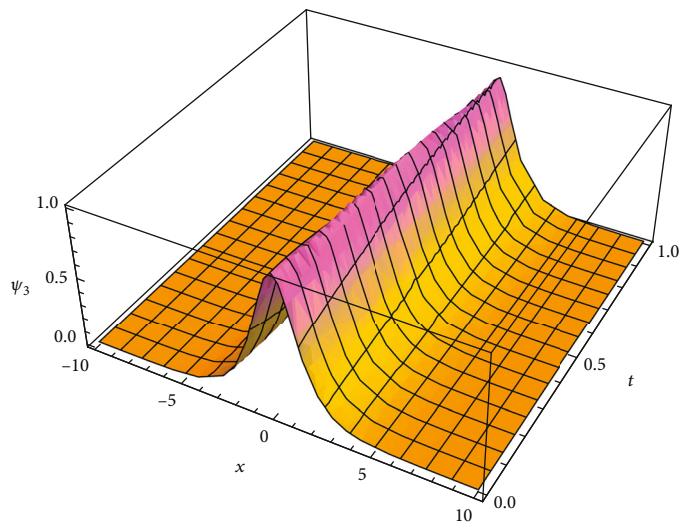

(a)

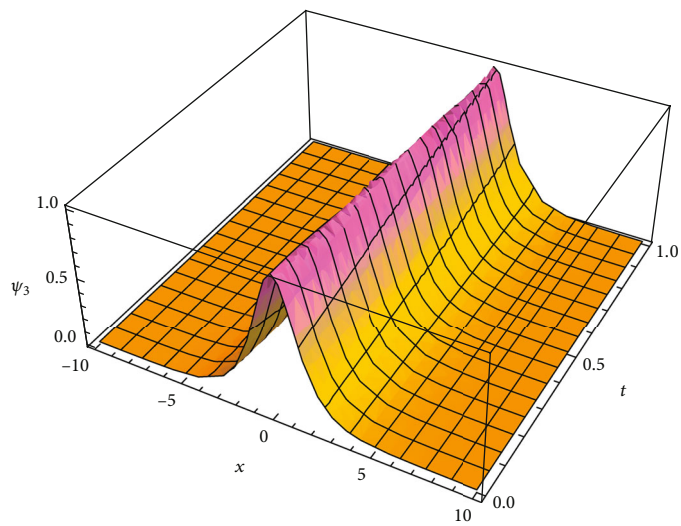

(b)

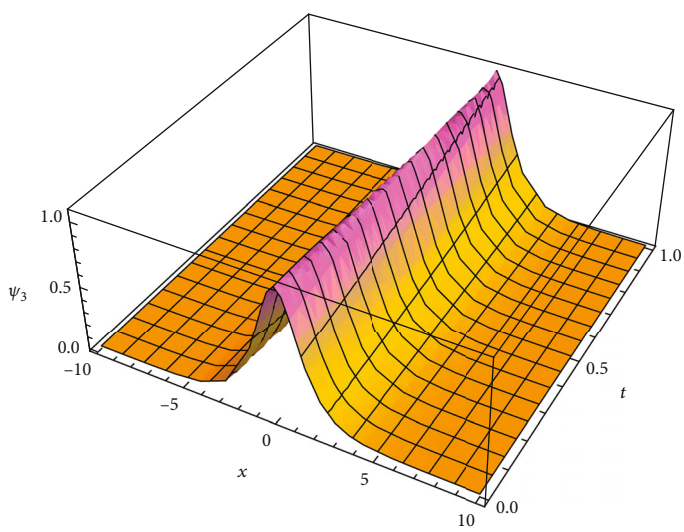

(c)

Figure 1: Continued.

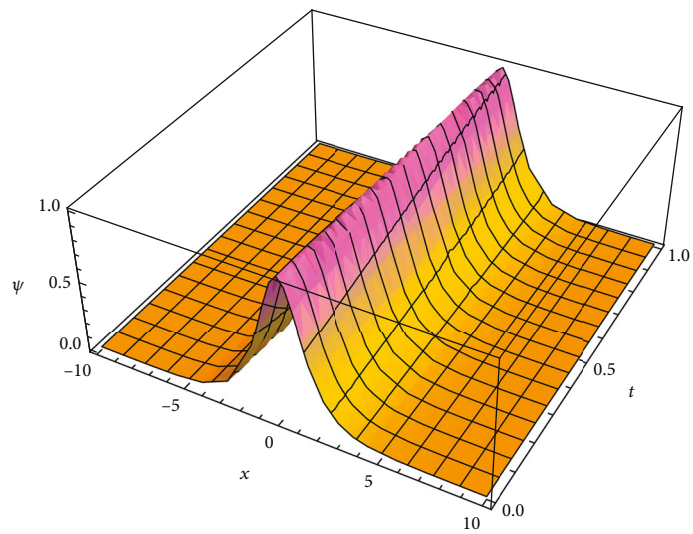

(d)

Figure 1: The graph of the exact solution $\psi(x,t)$ and the approximate solution $\psi_3(x,t)$ of Eq. (28): (a) $\psi_3(x,t)$ when $\alpha = 0.8$, (b) $\psi_3(x,t)$ when $\alpha = 0.90$, (c) $\psi_3(x,t)$ when $\alpha = 1$, and (d) $\psi(x,t)$ when $\alpha = 1$.

Table 1: Numerical comparisons between the 3rd approximate L-RPSM solution and the exact solution of Eq. (28) and the actual and relative errors when $x = 10$, $\alpha = 1$, $c = 1$, and $\omega = 0$.

t	$\psi_3(x,t)$	$\psi(x,t)$	Actual error	Relative error
0.01	0.917124×10^{-4}	0.917124×10^{-4}	1.51334×10^{-11}	1.65009×10^{-7}
0.02	0.926340×10^{-4}	0.926341×10^{-4}	1.21069×10^{-10}	1.30696×10^{-6}
0.04	0.945045×10^{-4}	0.945055×10^{-4}	9.68609×10^{-10}	1.02492×10^{-5}
0.08	0.983546×10^{-4}	0.983623×10^{-4}	7.75076×10^{-9}	7.87981×10^{-5}
0.16	0.106493×10^{-3}	0.106555×10^{-3}	6.20675×10^{-8}	5.82495×10^{-4}
0.32	0.124544×10^{-3}	0.125043×10^{-3}	4.98569×10^{-7}	3.98718×10^{-3}
0.64	0.168142×10^{-3}	0.172199×10^{-3}	4.05788×10^{-6}	2.35649×10^{-2}
0.70	0.177514×10^{-3}	0.182848×10^{-3}	5.33436×10^{-6}	2.91737×10^{-2}
0.80	0.194045×10^{-3}	0.202079×10^{-3}	8.03345×10^{-6}	3.9754×10^{-2}
0.90	0.211776×10^{-3}	0.223332×10^{-3}	1.15557×10^{-5}	5.17423×10^{-2}
1.00	0.230783×10^{-3}	0.246820×10^{-3}	1.60366×10^{-5}	6.49731×10^{-2}

$$g_3(x) = -\frac{2e^{x\omega}(e^{x\omega}-1)\omega^{11}}{(1+e^{x\omega})^7} \cdot \left(\left(1 - 32e^{x\omega} + 78e^{2x\omega} - 32e^{3x\omega} + e^{4x\omega}\right) + 12e^{x\omega}\left(1 - 4e^{x\omega} + e^{2x\omega}\right)\frac{\Gamma(1+2\alpha)}{\Gamma(1+\alpha)^2} \right). \tag{42}$$

Using the same procedures as in Application 6, we get the 3rd approximate L-RPS solution of Eq. (38) as follows:

$$\begin{aligned}\psi_3(x,t) = {} & \frac{-2\omega^2 e^{\omega x}}{(1+e^{\omega x})^2} + \frac{-2e^{\omega x}(e^{x\omega}-1)\omega^5}{(1+e^{\omega x})^3}\frac{t^{\alpha}}{\Gamma(1+\alpha)} \\ & + \frac{-2e^{\omega x}\left(1-4e^{\omega x}+e^{2\omega x}\right)\omega^8}{(1+e^{\omega x})^4}\frac{t^{2\alpha}}{\Gamma(1+2\alpha)} \\ & - \frac{2e^{x\omega}(e^{x\omega}-1)\omega^{11}}{(1+e^{x\omega})^7}\left(\left(1 - 32e^{x\omega} + 78e^{2x\omega} - 32e^{3x\omega} + e^{4x\omega}\right) + 12e^{x\omega}\left(1 - 4e^{x\omega} + e^{2x\omega}\right)\frac{\Gamma(1+2\alpha)}{\Gamma(1+\alpha)^2} \right)\frac{t^{3\alpha}}{\Gamma(1+3\alpha)}.\end{aligned} \tag{43}$$

It is worth mentioning that the solution in Eq. (43) matches the solution obtained in RPSM [23].

Table 2: Numerical results of the 3rd approximate L-RPSM solution of Eq. (28) at $\alpha = 0.80$ and $\alpha = 0.90$ and the corresponding residual error when $x = 10$, $c = 1$, and $\omega = 0$.

t	$\alpha = 0.80$		$\alpha = 0.90$	
	$\psi_3(x,t)$	Residual error	$\psi_3(x,t)$	Residual error
0.01	0.932888×10^{-4}	9.33684×10^{-5}	0.923098×10^{-4}	9.23369×10^{-5}
0.02	0.951850×10^{-4}	9.54255×10^{-5}	0.936394×10^{-4}	9.37336×10^{-5}
0.04	0.985919×10^{-4}	9.93154×10^{-5}	0.961753×10^{-4}	9.65016×10^{-5}
0.08	0.104845×10^{-3}	1.0701×10^{-4}	0.101098×10^{-3}	1.02224×10^{-4}
0.16	0.116721×10^{-3}	1.23148×10^{-4}	0.110953×10^{-3}	1.14808×10^{-4}
0.32	0.140545×10^{-3}	1.59391×10^{-4}	0.131735×10^{-3}	1.44774×10^{-4}
0.64	0.192924×10^{-3}	2.47494×10^{-4}	0.179596×10^{-3}	2.22943×10^{-4}
0.70	0.203721×10^{-3}	2.66307×10^{-4}	0.189666×10^{-3}	2.40237×10^{-4}
0.80	0.222526×10^{-3}	2.99316×10^{-4}	0.207315×10^{-3}	2.70925×10^{-4}
0.90	0.242424×10^{-3}	3.34448×10^{-4}	0.226116×10^{-3}	3.03988×10^{-4}
1.00	0.263508×10^{-3}	3.71783×10^{-4}	0.246156×10^{-3}	3.39491×10^{-4}

Remark 9. For $\alpha = 1$, a little focus while simplifying the series solution in Eq. (43) leads us to the exact solution of Eq. (38) in the following closed form:

$$\psi(x,t) = -\frac{2e^{\omega\left(x-\omega^2 t\right)}\omega^2}{\left(1+e^{\omega(x-\omega^2 t)}\right)^2}. \tag{44}$$

To confirm the efficiency of the L-RPS method and the accuracy of the ASS obtained with it, Figure 2 graphically shows the behavior of the solution and its compatibility with the exact solution in the case of $\alpha = 1$. It also shows the consistency of the solution's behavior with different values of α.

For more analysis of the results, numerical values for the actual and the relative errors of the approximation $\psi_3(x,t)$ are calculated in Table 3 when the $\alpha = 1$. Table 4 shows the residual error of the approximation $\psi_3(x,t)$ when $\alpha = 0.80$ and 0.90. The numerical results show that the obtained approximation is acceptable mathematically.

Application 10. Consider the nonlinear space-Caputo FKdV-BE

$$\begin{aligned}&\mathfrak{D}_t\psi(x,t) + \psi(x,t)\mathfrak{D}_x^{\beta}\psi(x,t) + \mathfrak{D}_x^2\psi(x,t) + \mathfrak{D}_x^3\psi(x,t)\\&\quad = 0, 0 < \beta \le 1, x, t > 0,\\&\psi(x,0) = x^3.\end{aligned} \tag{45}$$

In this application, the parameter values of Eq. (1) are $q = \epsilon = \eta = \mu = \alpha = 1$ while β is arbitrary in $(0,1]$ and the initial condition $\psi(x,0) = g_0(x) = x^3$. Depending on the steps of the L-RPSM, the form of Eq. (1) in Laplace space is

$$\begin{aligned}&\Psi(x,s) - \frac{x^3}{s} + \frac{1}{s}\mathscr{L}_t\left[\left(\mathscr{L}_t^{-1}[\Psi(x,s)]\right)^2\mathfrak{D}_x^{\beta}\left(\mathscr{L}_t^{-1}[\Psi(x,s)]\right)\right]\\&\quad + \frac{1}{s}\mathfrak{D}_x^2\Psi(x,s) + \frac{1}{s}\mathfrak{D}_x^3\Psi(x,s) = 0,\end{aligned} \tag{46}$$

the series solution of Eq. (46) is

$$\Psi(x,s) = \sum_{n=0}^{\infty}\frac{g_n(x)}{s^{n+1}}, x \in K, s > \delta \ge 0, \tag{47}$$

and the kth truncated series of $\Psi(x,s)$ is

$$\Psi_k(x,s) = \frac{x^3}{s} + \sum_{n=1}^{k}\frac{g_n(x)}{s^{n+1}}, k = 1, 2, \cdots. \tag{48}$$

According to the results in Eqs. (15), (18), and (20), we compute $g_n(x)$ for $n = 1$, 2, and 3 considering $\alpha = 1$ as

$$\begin{aligned}&g_1(x) = -\left(6 + 6x + r_1x^{6-\beta}\right),\\&g_2(x) = r_2x^{9-2\beta} + r_3x^{4-\beta} + r_4x^{3-\beta},\\&g_3(x) = -\left(r_5x^{12-3\beta} + r_6x^{7-2\beta} + r_7x^{6-2\beta} + r_8x^{2-\beta} + r_9x^{1-\beta} + r_{10}x^{-\beta}\right),\end{aligned} \tag{49}$$

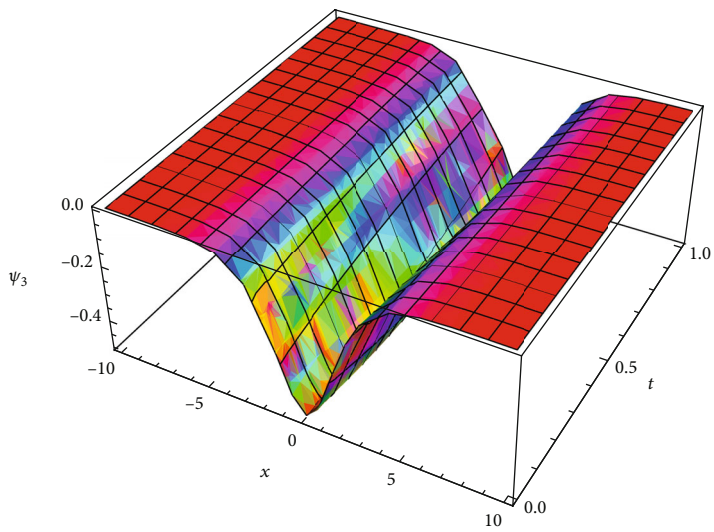

(a)

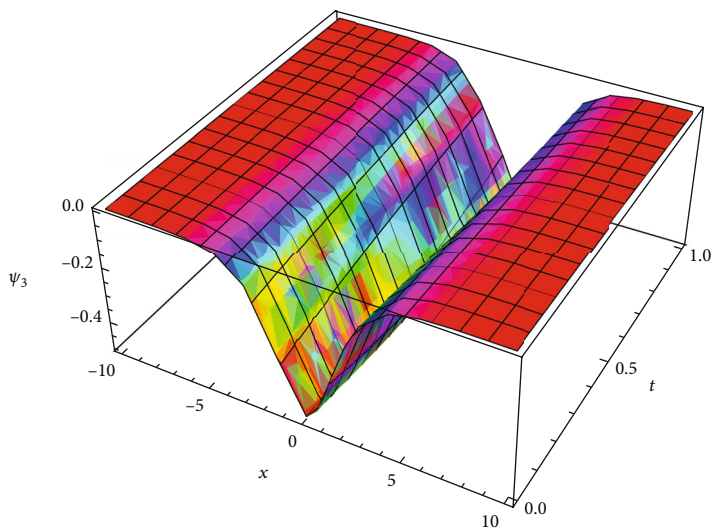

(b)

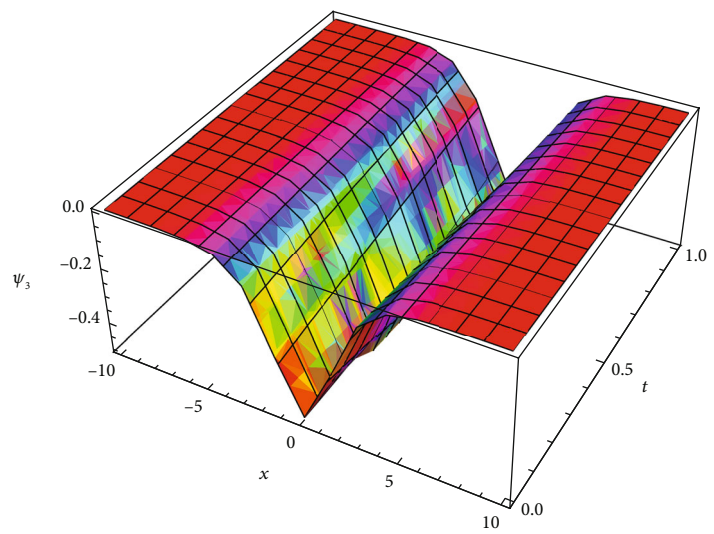

(c)

Figure 2: Continued.

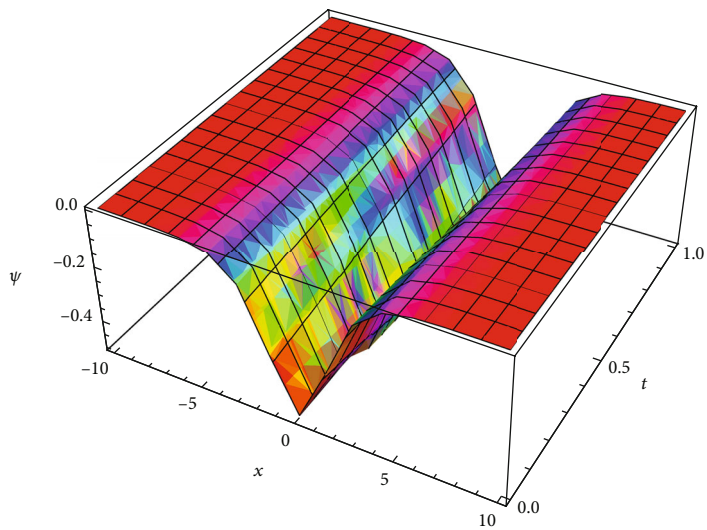

(d)

Figure 2: The graph of the exact solution $\psi(x,t)$ and the approximate solution $\psi_3(x,t)$ of Eq. (38): (a) $\psi_3(x,t)$ when $\alpha = 0.8$, (b) $\psi_3(x,t)$ when $\alpha = 0.90$, (c) $\psi_3(x,t)$ when $\alpha = 1$, and (d) $\psi(x,t)$ when $\alpha = 1$.

Table 3: Numerical comparisons between the 3rd approximate L-RPSM solution and the exact of Eq. (38) and the actual and relative errors when $x = 10$, $\alpha = 1$, and $\omega = 1$.

t	$\psi_3(x,t)$	$\psi(x,t)$	Actual error	Relative error
0.01	-0.91704×10^{-4}	-0.917040×10^{-4}	7.55689×10^{-17}	8.24052×10^{-13}
0.02	-0.926256×10^{-4}	-0.926256×10^{-4}	2.4223×10^{-15}	2.61515×10^{-11}
0.04	-0.944965×10^{-4}	-0.944965×10^{-4}	7.77739×10^{-14}	8.23035×10^{-10}
0.08	-0.983526×10^{-4}	-0.983526×10^{-4}	2.50549×10^{-12}	2.54745×10^{-8}
0.16	-0.106543×10^{-3}	-0.106543×10^{-3}	8.12640×10^{-11}	7.62732×10^{-7}
0.32	-0.125025×10^{-3}	-0.125027×10^{-3}	2.67257×10^{-9}	2.13759×10^{-5}
0.64	-0.172080×10^{-3}	-0.172171×10^{-3}	9.04760×10^{-8}	5.25502×10^{-4}
0.70	-0.182672×10^{-3}	-0.182815×10^{-3}	1.43158×10^{-7}	7.83074×10^{-4}
0.80	-0.201754×10^{-3}	-0.202038×10^{-3}	2.84229×10^{-7}	1.40681×10^{-3}
0.90	-0.222760×10^{-3}	-0.223282×10^{-3}	5.21702×10^{-7}	2.33652×10^{-3}
1.00	-0.245859×10^{-3}	-0.246759×10^{-3}	9.00116×10^{-7}	3.64776×10^{-3}

where

$$
\begin{aligned}
r_1 &= \frac{6}{\Gamma(4-\beta)},\\
r_2 &= r_1\frac{\Gamma(7-\beta)}{\Gamma(7-2\beta)} + r_1^2,\\
r_3 &= \frac{6}{\Gamma(2-\beta)} + 6r_1 + r_1(6-\beta)(5-\beta),\\
r_4 &= 6r_1 + r_1(6-\beta)(5-\beta)(4-\beta),\\
r_5 &= r_2\frac{\Gamma(10-2\beta)}{\Gamma(10-3\beta)} + r_1r_2 + 2r_1\left(r_2 - r_1^2\right),\\
r_6 &= r_3\frac{\Gamma(5-\beta)}{\Gamma(5-2\beta)} + r_1\frac{12}{\Gamma(2-\beta)} + 12\left(r_2 - r_1^2\right) + r_1r_3 + (8-2\beta)(9-2\beta)r_2,\\
r_7 &= r_4\frac{\Gamma(4-\beta)}{\Gamma(4-2\beta)} + 12\left(-r_1^2 + r_2\right) + r_1r_4 + (7-2\beta)(8-2\beta)(9-2\beta)r_2,\\
r_8 &= \frac{72}{\Gamma(2-\beta)} + (3-\beta)(4-\beta)r_3,\\
r_9 &= \frac{72}{\Gamma(2-\beta)} + (4-\beta)(3-\beta)(2-\beta)r_3 + (2-\beta)(3-\beta)r_4,\\
r_{10} &= (1-\beta)(2-\beta)(3-\beta)r_4.
\end{aligned}
\tag{50}
$$

Consequently, by considering the values of $r_1, \cdots, r_{10}$ in Eq. (50) and the form of the coefficients in Eq. (49), the 3rd approximate L-RPS solution of Eq. (45) is given by

Table 4: Numerical results of the 3rd approximate L-RPSM solution of Eq. (38) at $\alpha = 0.80$ and $\alpha = 0.90$ and the corresponding residual error when $x = 10$ and $\omega = 1$.

t	$\alpha = 0.80$		$\alpha = 0.90$	
	$\psi_3(x,t)$	Residual error	$\psi_3(x,t)$	Residual error
0.01	-0.932805×10^{-4}	4.54764×10^{-12}	-0.923013×10^{-4}	4.21998×10^{-13}
0.02	-0.951785×10^{-4}	4.17935×10^{-11}	-0.936312×10^{-4}	5.11727×10^{-12}
0.04	-0.985957×10^{-4}	3.84107×10^{-10}	-0.961697×10^{-4}	6.20559×10^{-11}
0.08	-0.104905×10^{-3}	3.53048×10^{-9}	-0.101112×10^{-3}	7.52597×10^{-10}
0.16	-0.117081×10^{-3}	3.24555×10^{-8}	-0.111095×10^{-3}	9.12871×10^{-9}
0.32	-0.142500×10^{-3}	2.98464×10^{-7}	-0.132721×10^{-3}	1.10764×10^{-7}
0.64	-0.203308×10^{-3}	2.74685×10^{-6}	-0.186083×10^{-3}	1.34502×10^{-6}
0.70	-0.186083×10^{-3}	1.34502×10^{-6}	-0.197934×10^{-3}	1.85763×10^{-6}
0.80	-0.240277×10^{-3}	5.61434×10^{-6}	-0.219180×10^{-3}	3.00573×10^{-6}
0.90	-0.265979×10^{-3}	8.18877×10^{-6}	-0.242431×10^{-3}	4.59547×10^{-6}
1.00	-0.242431×10^{-3}	4.59547×10^{-6}	-0.267845×10^{-3}	6.71891×10^{-6}

$$\psi_3(x,t) = x^3 - \left(6 + 6x + r_1 x^{6-\beta}\right)t + \left(r_2 x^{9-2\beta} + r_3 x^{4-\beta} + r_4 x^{3-\beta}\right)\frac{t^2}{2!} - \left(\left(r_5 x^{12-3\beta} + r_6 x^{7-2\beta} + r_7 x^{6-2\beta} + r_8 x^{2-\beta} + r_9 x^{1-\beta} + r_{10} x^{-\beta}\right)\right)\frac{t^3}{3!}. \tag{51}$$

Figure 3 shows a simulation of the solution of Eq. (45) on $(0,1] \times [0,1]$ in 3D space. Additionally, it displays the approximate solution $\psi_3(x,t)$ on the domain $(0,1] \times [0,1]$ for several values of $\beta = 0.4$, $\beta = 0.6$, $\beta = 0.8$, and $\beta = 1$.

We noticed from Figures 3(a)–3(d) that while each surface almost agrees well in its behavior, the representations of the surface graph solutions decrease steadily as the values of t and x increase in the definite domain. Also, the space-CFD plays a consistent role in the solutions.

Application 11. Consider the following nonlinear time-space-Caputo FKdV-BE

$$\begin{aligned} &\mathfrak{D}_t^{\alpha}\psi(x,t) + \psi(x,t)\mathfrak{D}_x^{\beta}\psi(x,t) + \mathfrak{D}_x^2\psi(x,t) \\ &\quad + \mathfrak{D}_x^3\psi(x,t) = 0, 0 < \alpha \le 1, 0 < \beta \le 1, x, t > 0, \\ &\quad \psi(x,0) = x. \end{aligned} \tag{52}$$

Comparing Eq. (52) with Eq. (1), we find that $q = \epsilon = \eta = \mu = 1$ with the initial condition $g_0(x) = x$. As a result, using the methodology described in Section 3, the LT of Eq. (52) is

$$\begin{aligned} &\Psi(x,s) - \frac{x}{s} + \frac{1}{s^{\alpha}}\mathscr{L}_t\left[\mathscr{L}_t^{-1}[\Psi(x,s)]\mathfrak{D}_x^{\beta}\left(\mathscr{L}_t^{-1}[\Psi(x,s)]\right)\right] \\ &\quad + \frac{1}{s^{\alpha}}\mathfrak{D}_x^2\Psi(x,s) + \frac{1}{s^{\alpha}}\mathfrak{D}_x^3\Psi(x,s) = 0, \end{aligned} \tag{53}$$

the series solution of Eq. (53) is

$$\Psi(x,s) = \sum_{n=0}^{\infty}\frac{g_n(x)}{s^{n\alpha+1}}, x \in K, s > \delta \ge 0, \tag{54}$$

and consequently the kth truncated series of $\Psi(x,s)$ will be

$$\Psi_k(x,s) = \frac{x}{s} + \sum_{n=1}^{k}\frac{g_n(x)}{s^{n\alpha+1}}, k = 1, 2, \cdots. \tag{55}$$

According to the results in Eqs. (15), (18), and (20), we derive $g_n(x)$ for $n = 1$, 2,and 3 as

$$\begin{aligned} g_1(x) &= -r_1 x^{2-\beta}, \\ g_2(x) &= r_2 x^{3-2\beta} + r_3 x^{-\beta} - \beta r_3 x^{-1-\beta}, \\ g_3(x) &= -\left(r_4 x^{4-3\beta} + r_5 x^{1-2\beta} + r_6 x^{-2\beta} + r_7 x^{-4-\beta} + r_8 x^{-3-\beta} + r_9 x^{-2-\beta}\right), \end{aligned} \tag{56}$$

where

$$r_1 = \frac{1}{\Gamma(2-\beta)},$$

$$r_2 = r_1^3(1-\beta) + r_1\frac{\Gamma(3-\beta)}{\Gamma(3-2\beta)},$$

$$r_3 = (2-\beta)(1-\beta)r_1,$$

$$r_4 = r_1^2(1-\beta)\left(r_2 - (1-\beta)r_1^3\right)\frac{\Gamma(1+2\alpha)}{\Gamma(1+\alpha)^2} + r_2\frac{\Gamma(4-2\beta)}{\Gamma(4-3\beta)} + r_2 r_1^2(1-\beta),$$

$$r_5 = r_3 r_1^2(1-\beta) + r_3\frac{\Gamma(1-\beta)}{\Gamma(1-2\beta)} + 2r_2(1-\beta)(3-2\beta),$$

$$r_6 = 2r_2(1-\beta)(3-2\beta)(1-2\beta) - r_3 r_1^2\beta(1-\beta) - 2r_3\beta\frac{\Gamma(1-\beta)}{\Gamma(1-2\beta)},$$

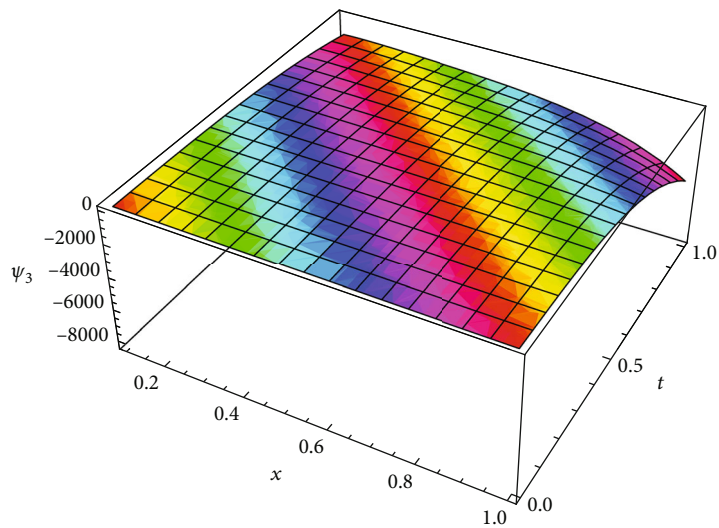

(a)

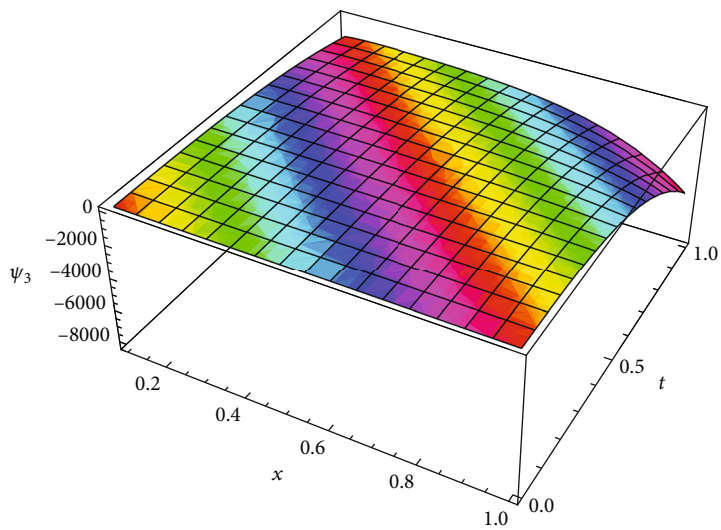

(b)

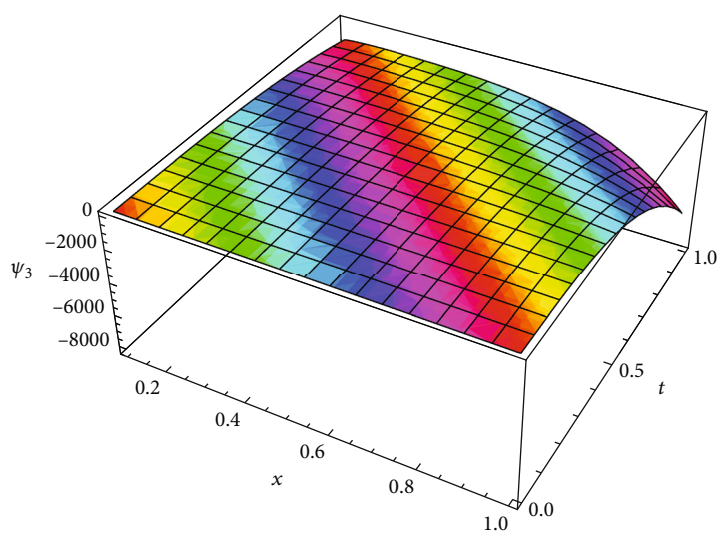

(c)

Figure 3: Continued.

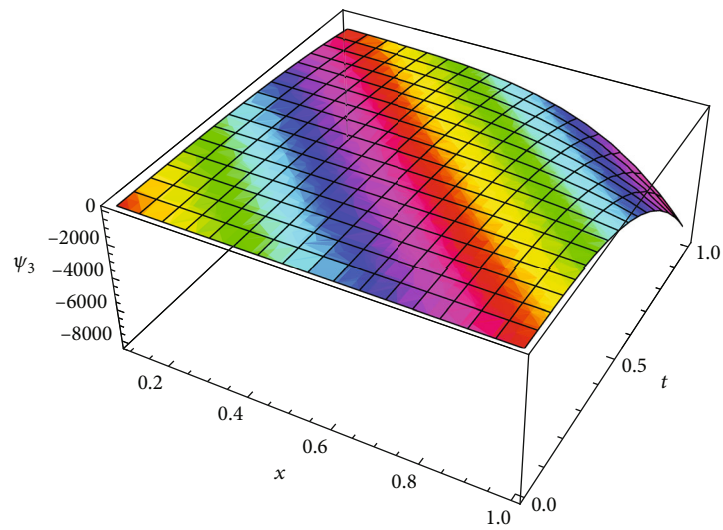

(d)

Figure 3: The graph of the approximate solution $\psi_3(x,t)$ of Eq. (41) when (a) $\beta = 0.4$, (b) $\beta = 0.6$, (c) $\beta = 0.8$, and (d) $\beta = 1$.

$$r_7 = r_3\beta(1+\beta)(2+\beta)(3+\beta),$$
$$r_8 = -2r_3\beta(1+\beta)(2+\beta),$$
$$r_9 = r_3\beta(1+\beta). \tag{57}$$

Consequently, by considering the values of $r_1, \cdots, r_9$ in Eq. (57), the 3rd approximate L-RPS solution of Eq. (52) is given as

$$\begin{aligned}\psi_3(x,t) = {} & x - r_1 x^{2-\beta}\frac{t^{\alpha}}{\Gamma(1+\alpha)} \\ & + \left(r_2 x^{3-2\beta} + r_3 x^{-\beta} - \beta r_3 x^{-1-\beta}\right)\frac{t^{2\alpha}}{\Gamma(1+2\alpha)} \\ & - \left(r_4 x^{4-3\beta} + r_5 x^{1-2\beta} + r_6 x^{-2\beta}\right. \\ & \left. + r_7 x^{-4-\beta} + r_8 x^{-3-\beta} + r_9 x^{-2-\beta}\right)\frac{t^{3\alpha}}{\Gamma(1+3\alpha)}.\end{aligned} \tag{58}$$

The advantage of the L-RPSM is that it is possible to pick any point in the integration domain and as well the ASS and all its time-space-CFDs will be applicable. In other words, it is possible to find a continuous ASS in which the ASS is continuously dependent on the time-space-CFD. Our next objective is to graphically illustrate the mathematical behavior of the approximate solution of Eq. (52) and its time-space-CFD geometrically. To do so, we plot the surface graph of the approximate solution $\psi_3(x,t)$ when $(\alpha,\beta) = (0.5,0.5)$, $(\alpha,\beta) = (1,0.5)$, $(\alpha,\beta) = (0.5,1)$, and $(\alpha,\beta) = (1,1)$ on the domain $(0,1] \times (0,1]$ as shown in Figure 4.

5. Conclusion

The L-RPS technique has been used in this study to find an ASS to the Caputo FKdV-BE. Three well-known physical applications are examined to confirm the applicability and superiority of the proposed strategy. In this technique, the FRPS is modified by coupling it to the LT operator. The advantage of using the L-RPSM is that it provides a more accurate convergence of the McLaurin series and requires a few computations without discretization, perturbation, or other physical restriction conditions. We explained the obtained ASS using graphics and numerical simulation, and they were compared with other well-known techniques in the literature. Consequently, the results confirm that the L-RPSM approach is straightforward for handling a variety of nonlinear FPDEs that might occur in engineering and scientific problems.

The main algorithm of L-RPSM for solving FKdV-BE of Eq. (1) can be summarized by the following steps:

(i) Applying the Laplace transform to the FKdV-BE

(ii) Using the Laurent series expansion to represent the solution of Laplace FKdV-BE in a new space. The coefficients of this expansion are determined in a similar way to the RPS method but with a new vision and a new analysis

(iii) Applying the inverse Laplace transform in step (ii), then we obtain a solution to this problem in the original space

The main advantages of LRPSM are as follows:

(i) It enables us to use the Laplace transform to solve nonlinear equations, while that was limited to linear equations only

(ii) It simplifies the processing of fractional differential equations by converting them to algebraic equations

(iii) Iterations can be calculated simply by functions built into any mathematical software using the

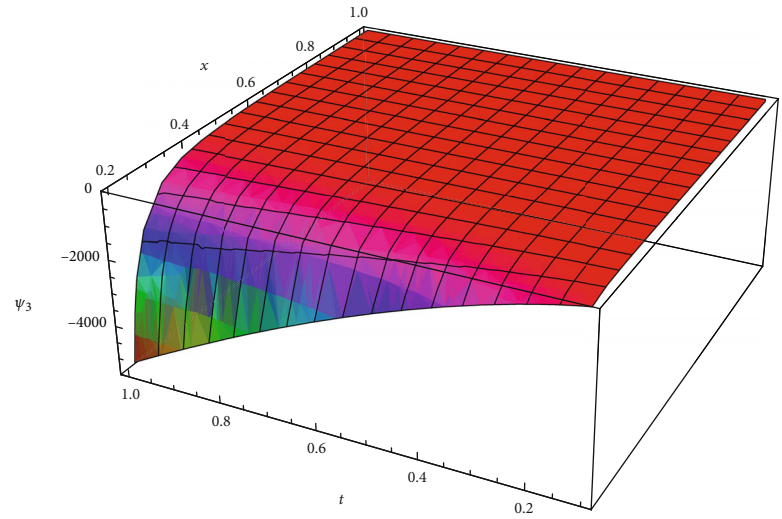

(a)

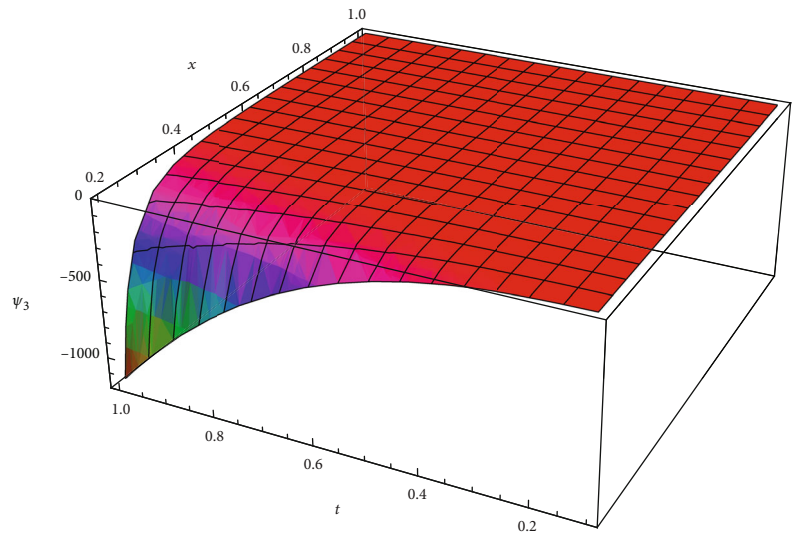

(b)

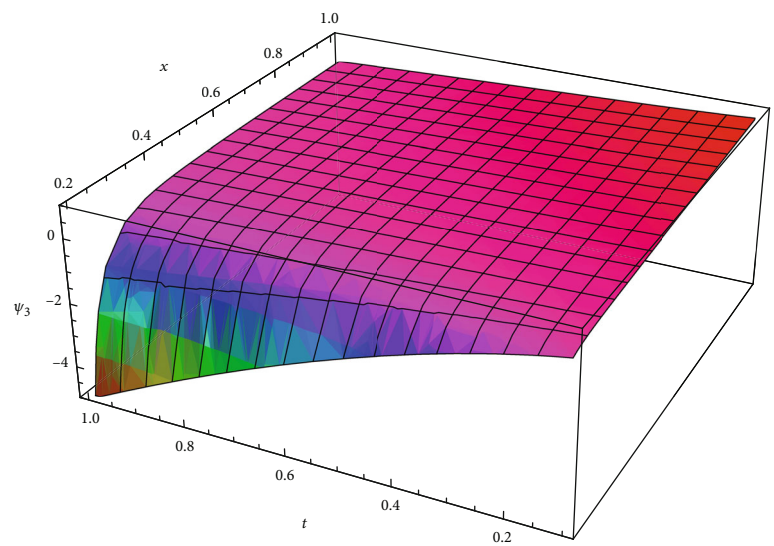

(c)

Figure 4: Continued.

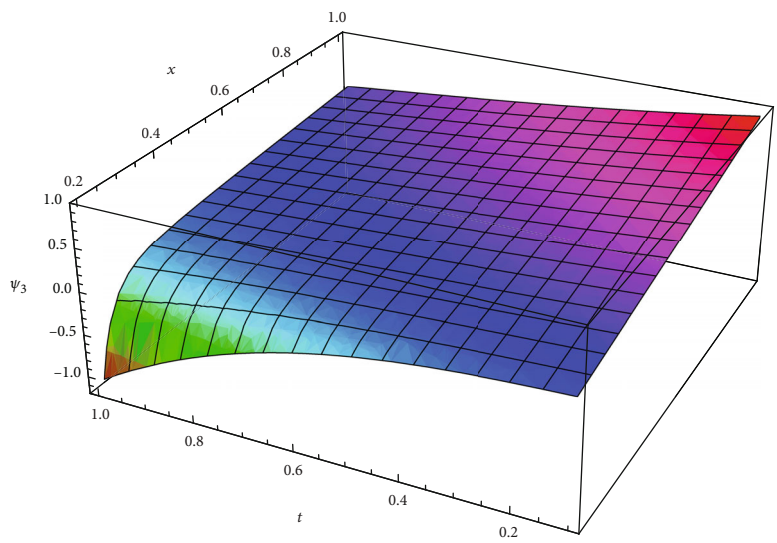

(d)

Figure 4: The surface graph of the 3rd approximate L-RPS solution of Eq. (52) is given as follows when (a) $(\alpha, \beta) = (0.5,0.5)$, (b) $(\alpha, \beta) = (1,0.5)$ (c) $(\alpha, \beta) = (0.5,1)$, and (d) $(\alpha, \beta) = (1, 1)$.

concept of limit at infinity, and unlike RPS, they do not require the derivative at each iteration

(iv) It does not require modeling assumptions, such as linearization, perturbation, or discretization

Thus, in future studies, the L-RPSM approach may be extended to find exact ASSs to other equations or model types that represent real-life phenomena, such as fractional integral equations, algebraic equations, and differential equations with boundary conditions instead of initial conditions, a new modified fractional Nagumo equation [33], spatiotemporal dynamic systems of interacting biological and chemical species [34], high-dimensional chaotic Lorenz system [35], generalize Hirota-Satsuma coupled KdV and MKdV equations [36], time-fractional vibration model of large membranes [37, 38], and fractional Black–Scholes option pricing equations [39].

Abbreviations

KdV-BE: The KdV-Burgers equation
PDEs: Partial differential equations
CFD: Caputo fractional derivative
ASSs: Analytical approximate series solutions
L-RPSM: Laplace residual power series method
LT: Laplace transform
RPSM: Residual power series method
F-PDEs: Fractional partial differential equations.

Data Availability

There is no underlying data used to support the results and conclusion in the paper.

Conflicts of Interest

The authors declare that they have no known competing financial interests or personal relationships that could appear to influence the work reported in this paper.

Acknowledgments

Aliaa Burqan was supported by the Department of Mathematics, Zarqa University, Zarqa, Jordan.

References

[1] H. Sun, Y. Zhang, D. Baleanu, W. Chen, and Y. Chen, "A new collection of real world applications of fractional calculus in science and engineering," *Communications in Nonlinear Science and Numerical Simulation*, vol. 64, pp. 213–231, 2018.

[2] G. S. Teodoro, J. T. Machado, and E. C. De Oliveira, "A review of definitions of fractional derivatives and other operators," *Journal of Computational Physics*, vol. 388, pp. 195–208, 2019.

[3] A. A. Kilbas, H. M. Srivastava, and J. J. Trujillo, *Theory and Applications of Fractional Differential Equations*, Elsevier, 2006.

[4] A. Qazza, A. Burqan, and R. Saadeh, "Application of ARA-residual power series method in solving systems of fractional differential equations," *Mathematical Problems in Engineering*, vol. 2022, Article ID 6939045, 17 pages, 2022.

[5] T. Eriqat, A. El-Ajou, N. O. Moa'ath, Z. Al-Zhour, and S. Momani, "A new attractive analytic approach for solutions of linear and nonlinear neutral fractional pantograph equations," *Chaos, Solitons & Fractals*, vol. 138, article 109957, 2020.

[6] A. Burqan, A. El-Ajou, R. Saadeh, and M. Al-Smadi, "A new efficient technique using Laplace transforms and smooth expansions to construct a series solution to the time-

fractional Navier-Stokes equations," *Alexandria Engineering Journal*, vol. 61, no. 2, pp. 1069–1077, 2022.

[7] K. Hosseini, M. Ilie, M. Mirzazadeh et al., "An effective computational method to deal with a time-fractional nonlinear water wave equation in the Caputo sense," *Mathematics and Computers in Simulation*, vol. 187, pp. 248–260, 2021.

[8] A. El-Ajou, "Adapting the Laplace transform to create solitary solutions for the nonlinear time-fractional dispersive PDEs via a new approach," *The European Physical Journal Plus*, vol. 136, no. 2, p. 229, 2021.

[9] A. El-Ajou and Z. Al-Zhour, "A vector series solution for a class of hyperbolic system of Caputo time-fractional partial differential equations with variable coefficients," *Frontiers in Physics*, vol. 9, article 525250, 2021.

[10] T. Eriqat, M. A. Oqielat, Z. Al-Zhour, A. El-Ajou, and A. S. Bataineh, "Revisited Fisher's equation and logistic system model: a new fractional approach and some modifications," *International Journal of Dynamics and Control*, vol. 11, no. 2, pp. 555–563, 2023.

[11] M. A. N. Oqielat, T. Eriqat, Z. Al-Zhour, O. Ogilat, A. El-Ajou, and I. Hashim, "Construction of fractional series solutions to nonlinear fractional reaction–diffusion for bacteria growth model via Laplace residual power series method," *International Journal of Dynamics and Control*, vol. 11, no. 2, pp. 520–527, 2023.

[12] R. Saadeh, A. Burqan, and A. El-Ajou, "Reliable solutions to fractional Lane-Emden equations via Laplace transform and residual error function," *Alexandria Engineering Journal*, vol. 61, no. 12, pp. 10551–10562, 2022.

[13] N. O. Moa'ath, A. El-Ajou, Z. Al-Zhour, T. Eriqat, and M. Al-Smadi, "A new approach to solving fuzzy quadratic Riccati differential equations," *International Journal of Fuzzy Logic and Intelligent Systems*, vol. 22, no. 1, pp. 23–47, 2022.

[14] D. J. Korteweg and G. de Vries, "XLI.On the change of form of long waves advancing in a rectangular canal, and on a new type of long stationary waves," *The London, Edinburgh, and Dublin Philosophical Magazine and Journal of Science*, vol. 39, no. 240, pp. 422–443, 1895.

[15] C. H. Su and C. S. Gardner, "Korteweg-de Vries equation and generalizations. III. Derivation of the Korteweg-de Vries equation and Burgers equation," *Journal of Mathematical Physics*, vol. 10, no. 3, pp. 536–539, 1969.

[16] K. Maleknejad, E. Babolian, A. J. Shaerlar, and M. Jahnagir, "Operational matrices for solving Burgers equation by using block-pulse functions with error analysis," *Australian Journal of Basic and Applied Sciences*, vol. 5, no. 12, pp. 602–609, 2011.

[17] A. H. Bhrawy, M. A. Zaky, and D. Baleanu, "New numerical approximations for space-time fractional Burgers' equations via a Legendre spectral-collocation method," *Romanian Reports In Physics*, vol. 67, no. 2, pp. 340–349, 2015.

[18] Q. Wang, "Homotopy perturbation method for fractional KdV-Burgers equation," *Chaos, Solitons & Fractals*, vol. 35, no. 5, pp. 843–850, 2008.

[19] A. K. Golmankhaneh, A. K. Golmankhaneh, and D. Baleanu, "Homotopy perturbation method for solving a system of Schrödinger-Korteweg-de Vries equations," *Romanian Reports In Physics*, vol. 63, no. 3, pp. 609–623, 2011.

[20] M. Wang, "Exact solutions for a compound KdV-Burgers equation," *Physics Letters A*, vol. 213, no. 5-6, pp. 279–287, 1996.

[21] M. M. Hassan, "Exact solitary wave solutions for a generalized KdV–Burgers equation," *Chaos, Solitons & Fractals*, vol. 19, no. 5, pp. 1201–1206, 2004.

[22] A. A. Soliman, "Exact solutions of KdV–Burgers' equation by exp-function method," *Chaos, Solitons & Fractals*, vol. 41, no. 2, pp. 1034–1039, 2009.

[23] A. El-Ajou, O. A. Arqub, and S. Momani, "Approximate analytical solution of the nonlinear fractional KdV–Burgers equation: a new iterative algorithm," *Journal of Computational Physics*, vol. 293, pp. 81–95, 2015.

[24] D. Kaya, "An application of the decomposition method for the KdVB equation," *Applied Mathematics and Computation*, vol. 152, no. 1, pp. 279–288, 2004.

[25] S. Momani, "Non-perturbative analytical solutions of the space- and time-fractional burgers equations," *Chaos, Solitons & Fractals*, vol. 28, no. 4, pp. 930–937, 2006.

[26] R. J. Cheng and Y. M. Cheng, "A meshless method for the compound KdV-Burgers equation," *Chinese Physics B*, vol. 20, no. 7, article 070206, 2011.

[27] H. N. Ismail, T. M. Rageh, and G. S. E. Salem, "Modified approximation for the KdV–Burgers equation," *Applied Mathematics and Computation*, vol. 234, pp. 58–62, 2014.

[28] M. Inc, "The approximate and exact solutions of the space- and time-fractional burgers equations with initial conditions by variational iteration method," *Journal of Mathematical Analysis and Applications*, vol. 345, no. 1, pp. 476–484, 2008.

[29] S. Momani, Z. Odibat, and A. Alawneh, "Variational iteration method for solving the space- and time-fractional KdV equation," *Numerical Methods for Partial Differential Equations*, vol. 24, no. 1, pp. 262–271, 2008.

[30] E. F. Doungmo Goufo, H. M. Tenkam, and M. Khumalo, "A behavioral analysis of KdVB equation under the law of Mittag–Leffler function," *Solitons & Fractals*, vol. 125, pp. 139–145, 2019.

[31] S. Rashid, A. Khalid, S. Sultana, Z. Hammouch, R. Shah, and A. M. Alsharif, "A novel analytical view of time-fractional Korteweg-de Vries equations via a new integral transform," *Symmetry*, vol. 13, no. 7, p. 1254, 2021.

[32] I. Podlubny, "Fractional differential equations," *Mathematics in Science and Engineering*, vol. 198, pp. 41–119, 1999.

[33] K. M. Saad, S. Deniz, and D. Baleanu, "On a new modified fractional analysis of Nagumo equation," *International Journal of Biomathematics*, vol. 12, no. 3, article 1950034, 2019.

[34] M. Alqahtai, K. M. Owolabi, K. M. Saad, and E. Pendza, "Spatiotemporal chaos in spatially extended fractional dynamical systems," *Communications in Nonlinear Science and Numerical Simulation*, vol. 119, article 107118, 2023.

[35] M. Alqahtai, M. Khader, and K. M. Saad, "Numerical simulation for a high-dimensional chaotic Lorenz system based on Gegenbauer wavelet polynomials," *Math*, vol. 11, no. 2, p. 472, 2023.

[36] R. M. Jena, S. Chakraverty, and D. Baleanu, "Solitary wave solution for a generalized Hirota-Satsuma coupled KdV and MKdV equations: a semi-analytical approach," *Alexandria Engineering Journal*, vol. 59, no. 5, pp. 2877–2889, 2020.

[37] R. M. Jena, S. Chakraverty, S. K. Jena, and H. M. Sedighi, "Analysis of time-fractional fuzzy vibration equation of large membranes using double parametric based residual power series method," *Journal of Applied Mathematics and Mechanics*, vol. 101, no. 4, article e202000165, 2021.

[38] R. M. Jena and S. Chakraverty, "Residual power series method for solving time-fractional model of vibration equation of large membranes," *Journal of Applied and Computational Mechanics*, vol. 5, no. 4, pp. 603–615, 2019.

[39] R. M. Jena and S. Chakraverty, "A new iterative method based solution for fractional Black–Scholes option pricing equations (BSOPE)," *SN Applied Sciences*, vol. 1, no. 1, p. 95, 2019.